MOISTURE CONTENT-WATER POTENTIAL RELATIONSHIP OF SUGAR MAPLE AND WHITE SPRUCE WOOD FROM GREEN TO DRY CONDITIONS

Maurice Defo
Graduate student

Yves Fortin
Professor

and

Alain Cloutier
Assistant professor

Département des sciences du bois et de la forêt
Faculté de foresterie et de géomatique
Université Laval
Québec, Qc, Canada, G1K 7P4

(Received March 1998)

ABSTRACT

The moisture content-water potential relationship was determined at 40°C and 60°C for sugar maple (*Acer saccharum* Marsh.) sapwood and at 60°C for white spruce (*Picea glauca* (Moench.) Voss.) heartwood from green to dry conditions. The pressure membrane technique was used for high moisture contents and equilibration over salt solutions for low moisture contents. The results show that at high moisture contents, the equilibrium moisture contents obtained from the green condition are lower than those obtained from full saturation (boundary desorption). It is recommended that the sorption history must be taken into account when modeling wood drying. Water potential at a given moisture content increases with temperature. There is a characteristic plateau in the green moisture content-water potential relationship obtained for sugar maple at water potentials between −2,000 and −6,000 J kg^{-1}, which can be attributed to its heterogeneous capillary structure. The maximum concentration of effective pore radius occurs at 0.02 μm in the case of sugar maple, corresponding to the size of the pit membrane openings.

Keywords: Water potential, sugar maple, white spruce, pore size distribution.

INTRODUCTION

A particular problem occurring when someone is preparing to model the moisture movement in wood during drying is the choice of the driving force. Different potentials are advocated in the literature. Moschler and Martin (1968), Nadler et al. (1985), and Cunningham et al. (1989) used the gradient in moisture content as the driving force. Comini and Lewis (1976), Thomas et al. (1980), and Irudayaraj et al. (1990) presented models of heat and mass transfer in wood based on the concept of moisture potential, which was first stated by Luikov (1966). Following Babbit (1950), the use of a thermodynamic potential function characterizing the energy status of water in wood has gained a wider acceptance during the last twenty years. In fact, its space derivative gives a force. The function used is either the gradient in chemical potential (Kawai et al. 1978; Siau 1983; Skaar and Kuroda 1985; Stanish et al. 1986; Skaar 1988; Siau 1992) or the gradient in water potential (Fortin 1979; Cloutier et al. 1992; Cloutier and Fortin 1994; Siau 1995). In the multi-component model proposed by Whitaker (1977), different driv-

Wood and Fiber Science, 31(1), 1999, pp. 62–70

ing forces are used, depending on the state of the water in wood. For water in the liquid, gaseous, and bound states, driving forces are, respectively, the gradient in pressure within the liquid, the gradient in total pressure, and the gradient in moisture content or in chemical potential (Plumb et al. 1985; Stanish et al. 1986; Perré 1987; Perré and Degiovanni 1990).

The water potential is the difference between the specific Gibbs free energy of water in the state under consideration and the specific Gibbs free energy of water in the standard reference state (Fortin 1979). This approach is advantageous because it can be theoretically applied to water in wood in the three phases (liquid water, water vapor, and bound water). Therefore, a limited number of parameters are required to solve the equation of mass transfer in wood during drying, namely, the moisture content–water potential relationship and the effective water conductivity of wood. We retained this approach in our efforts to develop a wood drying model applicable to vacuum drying.

The determination of the relationship between wood moisture content, M, and water potential, ψ, as well as the factors affecting this relation, has been the object of several studies (Penner 1963; Stone and Scallan 1967; Viktorin and Čermák 1977; Fortin 1979; Cloutier and Fortin 1991; Hernández and Bizoň 1994; Tremblay et al. 1996). The techniques used were equilibration over saturated salt solutions for low M values, the tension plate, the pressure plate, pressure membrane, and centrifuge for high M values. Of particular interest are the results of Cloutier and Fortin (1994) for aspen. A strong hysteresis was found between the boundary desorption and absorption curves. Barkas (1936), Penner (1963), and Fortin (1979) reported the same phenomenon for beech, Sitka spruce, and western hemlock, respectively. The ink-bottle effect appears to be the primary cause of the hysteresis in the M–ψ curves at high M values. In order to quantify the impact of the hysteresis of the M–ψ relationship on the simulation

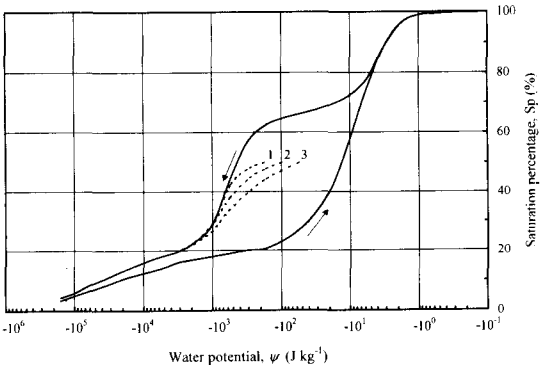

FIG. 1. Saturation percentage-water potential relationship of aspen sapwood along the boundary desorption and absorption curves at 20°C. 1, 2, and 3 represent the saturation percentage-water potential scanning curves used for simulation (adapted from Cloutier and Fortin 1994).

of convective drying of aspen sapwood, Cloutier and Fortin (1994) used three hypothetical scanning curves for an initial saturation percentage of 50% (Fig. 1). The simulation results reported show that differences in the predicted drying times as high as 25% can occur depending on the M–ψ curve used. In a previous study on sorption measurements, Goulet (1968) indicated that the M–ψ drainage curve starting from the green condition is similar in shape to the boundary drainage curve, but stands within the hystereris loop until a relative humidity of about 60% is reached. Since wood in nature is always in a state of sorption, it is important to consider the sorption history in the development of wood drying models.

The shape of the M–ψ curves at high M values changes markedly within and among species. This is related to the pore size distribution since water potential takes capillary forces into account (Fortin 1979). Cloutier and Fortin (1991) and Tremblay et al. (1996) reported an appreciable temperature effect on M–ψ curves. The ψ values increased with temperature at a given M. Possible causes are the dependence of surface tension of water on temperature, the effect of entrapped air, and the presence of surface active contaminants at the air-water interface (Chahal 1965; Saha and Tripathi 1981). It is also worth mentioning that

the wood structural direction has no effect on the M–ψ relationship as shown by Cloutier et al. (1995).

The purpose of this study is to determine the moisture content–water potential (M–ψ) relationship of sugar maple (*Acer saccharum* Marsh.) sapwood and white spruce (*Picea glauca* (Moench.) Voss.) heartwood from green to dry conditions. The effective pore size distribution of sugar maple is determined. The effect of temperature on M–ψ is also assessed. The M–ψ relationships determined in this study will be used to model mass transfer in wood during vacuum drying, under the hypothesis that the vacuum has no effect on the matric potential component of the total water potential.

MATERIAL AND METHODS

Material

The material used for this study was obtained from a natural stand located in the Beauce area, southeast of Québec City, Québec, Canada. Six trees for each species were felled in the early winter in the case of spruce, and in the late fall in the case of sugar maple. Specimens cut to 45 × 10 × 45 mm (L × R × T) and free of visual defects were obtained from spruce heartwood and sugar maple sapwood. The test specimens were then selected, matched, packed in groups of 12 (two from each tree), and stored at −15°C in polyethylene bags. Before each experiment, the specimens were kept over distilled water at 21°C in a closed desiccator for 24 hours to allow them to thaw.

The specific gravity (oven-dry weight/green volume) of sugar maple sapwood used in this study varied from 0.587 to 0.676, with an average initial moisture content of about 60%. For white spruce heartwood, the specific gravity varied from 0.318 to 0.427, with an average initial moisture content of about 35%.

Methods

The experiments were conducted at 40°C and 60°C for sugar maple and 60°C for white spruce. Two experimental techniques were used: the pressure membrane technique for high moisture contents and equilibration over saturated salt solutions for low moisture contents.

A detailed description of the pressure membrane apparatus and the heating system is given in Cloutier and Fortin (1991). The test specimens were placed on the porous membrane and pressed firmly against a 2-mm-thick clay layer formed on the porous membrane to ensure good hydraulic contact. The clay was first prepared at 60% moisture content for the tests with sugar maple and at 50% for the tests with spruce. This was to prevent the absorption of water by the specimens that would have occurred with saturated clay. The moisture content levels of the clay were determined from preliminary tests, which consisted of measuring the water uptake of specimens put in contact with clay at various degrees of saturation. Once the specimens were in place, the chamber was hermetically closed and the pressure applied gradually. When the outflow ceased or became negligible, the pressure was slowly released and the equilibrium M was determined by the gravimetric method.

The equilibration over saturated salt solutions was carried out using sorption vats described by Goulet (1968). Three saturated salt solutions were used: K_2SO_4 (R.H. = 96% at 60°C), KCl (R.H. = 80.7% at 60°C), and $NaNO_2$ (R.H. = 59.3% at 60°C). The saturated solutions and the wood specimens were enclosed in glass desiccators and put in water baths maintained at 60 ± 0.1°C. The specimens were placed above the solutions on plexiglas stands, allowing periodic weighing of the test specimens without opening the desiccators. When a constant weight was reached, the specimens were removed and their moisture content was determined. The overall process took 45 days for white spruce and two months for sugar maple.

RESULTS AND DISCUSSION

Green moisture content–water potential relationship

The results of the M–ψ determinations are summarized in Table 1 and are presented

TABLE 1. *Summary of the results of the M–ψ determinations.*

Temperature	Sugar maple						White spruce				
°C	Method[a]	R.H. %	ψ J kg^{-1}	M %	SE[b] %	dM/dψ %	Method	R.H. %	ψ J kg^{-1}	M %	SE %
60	PM	99.984	−24	54.8	1.6	—	PM	99.935	−100	31.5	0.4
	PM	99.980	−31	50.1	1.4	40.72	PM	99.606	−607	30.5	0.3
	PM	99.967	−50	46.1	0.9	12.67	PM	98.984	−1,570	29.5	0.1
	PM	99.908	−141	42.0	0.6	2.47	PM	96.705	−5,150	25.2	0.1
	PM	99.803	−303	39.0	0.4	1.03	K_2SO_4	96.000	−6,277	22.3	0.1
	PM	99.611	−600	37.3	0.4	0.48	KCl	80.700	−32,970	15.4	0.1
	PM	98.708	−2,000	34.0	0.3	0.11	$NaNO_2$	59.299	−80,345	8.4	0.1
	PM	96.706	−5,150	32.0	0.3	0.08					
	PM	96.079	−6,150	30.7	0.2	0.08					
	K_2SO_4	96.000	−6,277	30.6	0.2	0.08					
	KCl	80.700	−32,970	14.9	0.1	0.03					
	$NaNO_2$	59.300	−80,345	8.1	0.1	—					
40	PM	99.964	−52	53.6	1.3						
	PM	99.945	−80	49.5	0.8						
	PM	97.709	−3,350	36.6	0.3						

[a] PM = pressure membrane.
[b] SE = standard error based on 12 specimens.

graphically in Fig. 2 for sugar maple and in Fig. 3 for white spruce. The curves are plotted on a semi-logarithmic scale to avoid congestion of data points at high ψ values. The temperature coefficient of ψ at given M values obtained from the M–ψ relationship at 40°C and 60°C for sugar maple was used to extrapolate the M–ψ relationship at 21°C (Fig. 2), assuming a linear relationship between ψ and T. For comparison purposes, the boundary desorption curve for sugar maple (Fortin 1981; Hernández and Bizoň 1994) is also shown in Fig. 2, and the boundary desorption curve for Sitka spruce (Penner 1963), whose pore structure is similar to white spruce, is shown in Fig. 3.

As shown in Figs. 2 and 3, the M–ψ drainage curve obtained from the green condition is similar in shape to the M–ψ drainage curve obtained from the fully saturated state when water potential is less than -1×10^3 J kg^{-1}. For ψ values above -1×10^3 J kg^{-1}, the curves are different. The equilibrium moisture

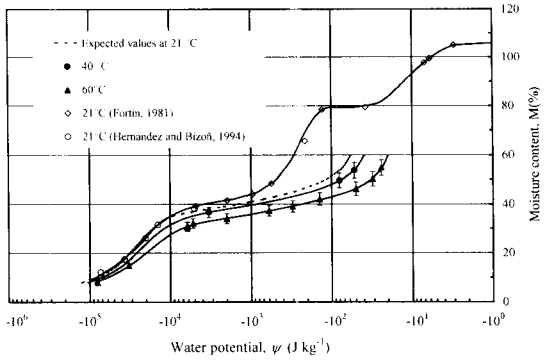

FIG. 2. Moisture content–water potential relationship of sugar maple sapwood at 40°C and 60°C from green to dry conditions and boundary drainage curve at 21°C (adapted from Fortin 1981 and Hernández and Bizoň 1994).

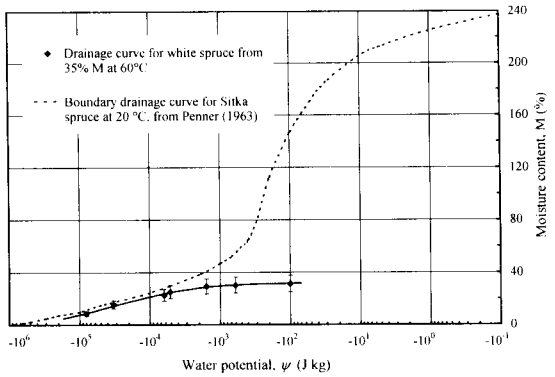

FIG. 3. Moisture content–water potential relationship for white spruce heartwood at 60°C from green to dry conditions and boundary desorption curve for Sitka spruce at 20°C (adapted from Penner 1963).

TABLE 2. *Experimental and calculated temperature coefficients for the M–ψ relationship of sugar maple and red pine.*

M %	Sugar maple ψ (at 60°C) J kg^{-1}	Sugar maple $\partial\psi/\partial T$ J kg^{-1} °C^{-1} Experimental	Sugar maple $\partial\psi/\partial T$ J kg^{-1} °C^{-1} Calculated	Red pine (from Tremblay et al. 1996) ψ (at 56°C) J kg^{-1}	Red pine (from Tremblay et al. 1996) $\partial\psi/\partial T$ J kg^{-1} °C^{-1} Experimental	Red pine (from Tremblay et al. 1996) $\partial\psi/\partial T$ J kg^{-1} °C^{-1} Calculated
60	−20	0.95	0.05	−630	3.21	1.67
50	−32	2.12	0.08	−742	6.33	1.91
40	−236	31.2	0.59	−1,020	14.3	2.93

contents (EMC) obtained from the green state are lower than those from full saturation. It may be expected that numerous drainage curves could be measured from the green condition due to the seasonal variation of M in standing trees (Linzon 1969). The practical implications are that, depending on the green M in the trees at the time of felling, and depending on whether M before felling is toward an increasing or a decreasing trend, the effectiveness of a given drainage or drying process may be quite different (Fortin 1979).

At a given M, ψ increases with temperature as shown in Fig. 2. The M–ψ curves are shifted to the right side. The effect of temperature on ψ has been described by several authors (Chahal 1965; Fortin 1979; Saha and Tripathi 1981; Cloutier and Fortin 1991). The matric potential is directly related to the equivalent matric pressure applied on the sample side of the porous membrane by the following relation:

$$\psi_m = -\bar{V}_w P_m \quad (1)$$

where ψ_m = matric potential (J kg^{-1}); $\bar{V}_w$ = specific volume of water (m^3 kg^{-1}); P_m = equivalent matric pressure (Pa). The relation existing between P_m and the capillary structure of wood is given by:

$$P_m = \frac{2\gamma}{r}\cos\theta \quad (2)$$

where γ = surface tension of water (N m^{-1}); r = effective radius of the capillary (m); θ = contact angle between the liquid and the surface of the capillary.

Substituting Eq. (2) into Eq. (1), we obtain:

$$\psi_m = -\bar{V}_w \frac{2\gamma}{r}\cos\theta \quad (3)$$

Equation (3) can be used in the determination of the pore size distribution of wood based on experimentally obtained ψ_m values. But, as mentionned by Siau (1995), it is probably not valid to estimate pore sizes at water potential values lower than −10,000 J kg^{-1} because the calculated radii (0.0135 μm and less at 60°C) approach the radius of the water molecule, 1.5 Å. The derivative of ψ_m with respect to temperature, assuming that the specific volume of water and the capillary radius are independent of temperature, leads to:

$$\left(\frac{\partial\psi_m}{\partial T}\right)_M = \psi_m \frac{1}{\gamma}\frac{\partial\gamma}{\partial T} \quad (4)$$

where $(\partial\psi_m/\partial T)_M$ = temperature coefficient of ψ_m at a constant moisture content (J kg^{-1} °C^{-1}).

The calculated values of the temperature coefficient of ψ_m based on Eq. (4) and experimental values based on data for sugar maple are presented in Table 2 for some arbitrary M values over 30%. The results of the temperature coefficient of ψ_m for red pine (Tremblay et al. 1996) are also presented in Table 2. Experimental values are several times higher than calculated values for both species. Cloutier and Fortin (1991) came to the same conclusion for aspen. This implies that the increase in ψ_m with temperature cannot be entirely explained by the dependence of the surface tension of water on temperature. Entrapped air (Chahal 1965) and surface active contaminants at the air-water interface (Saha and Tripathi 1981) were proposed to explain this behavior. The factors that may determine the amount of en-

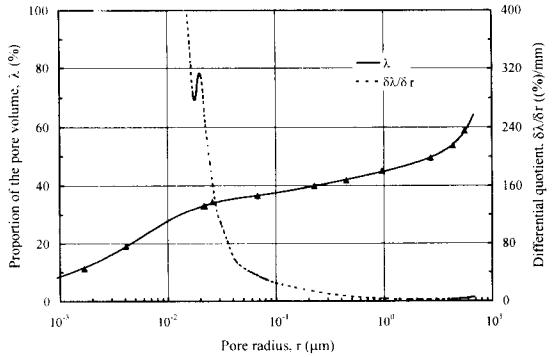

FIG. 4. Effective cumulative and differential pore size distribution of sugar maple sapwood as inferred from the moisture content–water potential relationship obtained at 60°C from green to dry conditions.

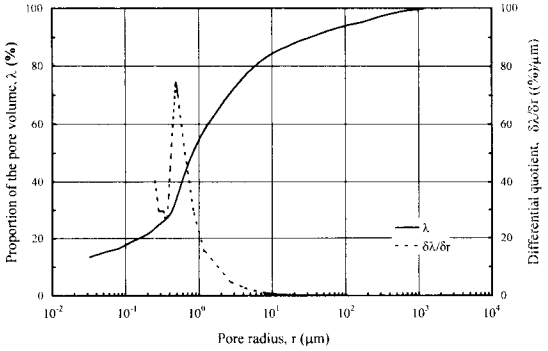

FIG. 5. Effective cumulative and differential pore size distribution of Sitka spruce as inferred from the moisture content–water potential relationship obtained at 20°C from fully saturated to dry conditions (Penner 1963).

trapped air are the pore size distribution and the initial moisture content (Fortin 1979).

There is a discrepancy between the predicted values of $(\partial\psi_m/\partial T)_M$ for sugar maple and red pine (Table 2). The difference observed can be mainly ascribed to the low initial moisture content of sugar maple and also to the fact that the M–ψ relationship is not the same for both species.

Effective pore size distribution

Equation (3) was used in the determination of the effective cumulative and differential pore size distributions, with the hypothesis of a zero contact angle. Figure 4 shows the proportion of pore volume and differential quotient plotted against the pore radius of sugar maple, based on the green M–ψ relationship obtained at 60°C. The proportion (%) of pore volume, λ, is the proportion of the pore volume occupied by pores whose radius is equal or smaller than a given radius, r. It was obtained by dividing the measured EMC by moisture content at full saturation (93%) for EMC values above FSP. For EMC values below FSP, shrinkage was taken into consideration in the calculation of the total pore volume as indicated below:

$$\lambda = \frac{M}{\frac{1}{G_m} - \frac{1}{G_{ws}}} \cdot 100 \qquad (5)$$

where G_m is the specific gravity of wood (oven-dry weight/moist volume); and G_{ws} is the specific gravity of the wood substance. If the function $\lambda = f(r)$ is differentiated, the effective distribution frequency of the pores is obtained. As suggested by Heizmann (1970), the local maxima on this curve indicate the region(s) where there is a large concentration of pore openings. Since the initial moisture content of white spruce was very low, the boundary desorption curve of Sitka spruce (Penner 1963) was used to establish its effective cumulative and differential pore size distribution (Fig. 5), only for comparison purposes.

As illustrated by the cumulative pore size distribution in Fig. 4, the desorption began when 34.5% of the total pore volume with an effective radius larger than 6.8 μm was empty. This includes all the vessel elements since 21% of the volume of sugar maple is constituted of vessels with a diameter ranging from 20 μm to 100 μm, interconnected by simple perforation plates (Panshin and de Zeeuw 1980). From the differential quotient (Fig. 4), a large proportion of the effective pore openings occurs in the range 0.018 μm to 0.2 μm, with a maximum at about 0.02 μm. This region corresponds to the pit membrane openings in fibers and ray parenchyma cells. Siau (1995) gives a range of pit membrane openings diameter from 0.005 μm to 0.17 μm, with

a log mean of 0.03 μm for hardwoods. The values we obtained are in the same order of magnitude. The large proportion of the effective pit membrane openings for Sitka spruce (Fig. 5) range from 0.37 μm to 4 μm with a maximum at about 0.5 μm. Petty (1970) measured pit membrane openings in Sitka spruce from electron micrographs. He reported openings 0.25 μm wide and 1 μm long with an equivalent diameter of 0.4 μm. Sébastian et al. (1965) calculated diameters from 1.4 μm to 5 μm, with an average of 2.6 μm from flow measurements in white spruce, while microscopic measurements yielded an average spacing between the microfibrillar strands of the margo of 1.3 μm for the same species. Tremblay et al. (1996) found the largest effective pit membrane openings at 0.2 μm for red pine. These results show that the pit membrane openings in hardwoods are one order of magnitude smaller than the values for softwoods.

The difference between the M–ψ relationships of hardwoods and softwoods can be explained by differences in their anatomical features. Hardwoods have a more complex structure than softwoods. According to Panshin and de Zeeuw (1980), sugar maple is constituted of 21% vessels, 61% fibers (including fiber tracheids and libriform fibers), and 17.9% ray parenchyma whereas softwoods are constituted of more than 90% tracheids.

It can be seen from Table 1 ($dM/d\psi$) that in the portion of the green M–ψ curves of sugar maple between water potentials of −2,000 and −6,000 J kg^{-1}, M decreases very slowly with a decrease in water potential. From this it may be inferred that water filling the fibers lumina has been removed and the remainder is held firmly by high capillary tension into pit openings in the fibers or in ray parenchyma as was pointed out by Hart (1984) and Wheeler (1982). The latter author noted that the parenchyma-parenchyma pit membranes are thicker than both the intervessel pit membranes and the fiber-fiber pit membranes, and consequently are less efficient pathways for liquid flow.

CONCLUSIONS

The purpose of this study was to determine the moisture content-water potential relationship of sugar maple sapwood and white spruce heartwood, from green to dry conditions. The experiments were conducted using the pressure membrane technique for high moisture contents and equilibration over saturated salt solutions for low moisture contents.

At high water potential values, the equilibrium moisture contents obtained when starting drainage from the green condition are lower than the values for the boundary drainage curve obtained from full saturation. The green moisture content–water potential relationship for sugar maple exhibits a characteristic plateau at water potentials between −2,000 and −6,000 J kg^{-1}. This can be explained by the effective pore size distribution of sugar maple wood.

The effective pore size distribution suggests that a large proportion of the pit membrane openings for sugar maple range from 0.015 μm to 0.2 μm with a maximum at 0.02 μm. The effective pit membrane openings for spruce range from 0.37 μm to 4 μm with a maximum at about 0.5 μm.

The measurements performed at 40°C for sugar maple, together with the measurements at 60°C, show that water potential at a given moisture content increases with temperature. Possible causes are the dependence of surface tension on temperature, entrapped air and the presence of surface active contaminants.

ACKNOWLEDGMENTS

This research project was supported by the Programme Pluri-annuel des Bourses Canada-Cameroun, the Ministère des Ressources Naturelles du Québec, and by the Natural Sciences and Engineering Research Council of Canada under grant no. OGP0121954.

REFERENCES

BABBIT, J. D. 1950. On the differential equations of diffusion. Can. J. Res. Sect. A. 28:449–474.

BARKAS, W. W. 1936. Wood-water relationship. 2. The fi-

ber saturation point of beech wood. Proc. Phys. Soc. 48:576–588.

CHAHAL, R. S. 1965. Effect of temperature and trapped air on matric suction. Soil Sci. 100:262–266.

CLOUTIER, A., AND Y. FORTIN. 1991. Moisture content-water potential relationship of wood from saturated to dry conditions. Wood Sci. Technol. 25:263–280.

———, AND ———. 1994. Wood drying modelling based on the water potential concept: Hysteresis effect. Drying Technol. 12(8):1793–1814.

———, ———, AND G. DHATT. 1992. A wood drying finite element model based on the water potential concept. Drying Technol. 10(5):1151–1181.

———, C. TREMBLAY, AND Y. FORTIN. 1995. Effect of specimen structural orientation on the moisture content-water potential relationship of wood. Wood Sci. Technol. 29:235–242.

COMINI, G., AND R. W. LEWIS. 1976. A numerical solution of two dimensional problems involving heat and mass transfer. Int. J. Heat Mass Transfer 19(12):1387–1392.

CUNNINGHAM, M. J., R. B. KEEY, AND C. KERDEMELIDIS. 1989. Isothermal moisture transfer coefficients in *Pinus radiata* above the fiber saturation point, using the moment method. Wood Fiber Sci. 21:112–122.

FORTIN, Y. 1979. Moisture content matric-potential relationship and water flow properties of wood at high moisture contents. Ph.D. thesis, The University of British Columbia, Vancouver, BC. 187 pp.

———. 1981. Relationships between water potential and equilibrium moisture content of sugar maple wood. Unpublished data.

GOULET, M. 1968. Phénomènes de second ordre de la sorption d'humidité dans le bois au terme d'un conditionnement de trois mois à température normale. Seconde partie: Essais du bois d'érable à sucre en compression radiale. Note de recherche n° 3, Département d'exploitation et utilisation du bois. Univ. Laval, Québec, Canada. 29 pp.

HART, C. A. 1984. Relative humidity, EMC, and collapse shrinkage in wood. Forest Prod. J. 34(11/12):45–54.

HEIZMANN, P. 1970. Die Bewegung von flüssigem Wasser in kapillarporösen Körpern unter dem Einfluss kapillarer Zugkräfte sowie dem Einfluss von Zentrifugalkräften. Holz Roh-u Werst. 28(8): 295–309. *Also:* Movement of liquid water in capillary porous bodies under the influence of capillary tension forces and centrifugal forces. Transl. No. 10466, CSIRO, Australia.

HERNÁNDEZ, R. E., AND M. BIZOŃ. 1994. Change in shrinkage and tangential compression strength of sugar maple below and above fiber saturation point. Wood Fiber Sci. 26(3):360–369.

IRUDAYARAJ, J., K. HAGHIGHI, AND R. L. STROSHINE. 1990. Nonlinear finite element analysis of coupled heat and mass transfer problems with an application to timber drying. Drying Technol. 8(4):731–749.

KAWAI, S., K. NAKATO, AND T. SADOH. 1978. Moisture movement in wood below the fiber saturation point. Mokuzai Gakkaishi 24(5):273–280.

LINZON, S. N. 1969. Seasonal water content and distribution in eastern white pine. Forestry Chron. 45(1):38–43.

LUIKOV, A. V. 1966. Heat and mass transfer in capillary-porous bodies. Pergamon Press, New York, NY. 523 pp.

MOSCHLER, W. W. JR., AND R. E. MARTIN. 1968. Diffusion equation solutions in experimental wood drying. Wood Sci. 1:47–56.

NADLER, K. C., E. T. CHOONG, AND T. M. WETZEL. 1985. Mathematical modeling of diffusion of water in wood during drying. Wood Fiber Sci. 17:404–423.

PANSHIN, A. J., AND C. DE ZEEUW. 1980. Textbook of wood technology. McGraw-Hill, New York, NY. 722 pp.

PENNER, E. 1963. Suction and its use as measure of moisture contents and potentials in porous materials. Pages 245–252 *in* A. Wexler, ed. Humidity and moisture, Vol. 4. Reinhold Publ. Co. New York, NY.

PERRÉ, P. 1987. Le séchage convectif des bois résineux. Choix, validation et utilisation d'un modèle. Thèse de Doctorat, Université de Paris VII, Paris, France. 251 pp.

———, AND A. DEGIOVANNI. 1990. Simulation par volumes finis des transferts couplés en milieux poreux anisotropes: séchage du bois à basse et à haute température. Int. J. Heat Mass Transfer 33(11):2463–2478.

PETTY, J. A. 1970. Permeability and structure of the wood of Sitka spruce. Proc: Royal Soc. Lond. B. 175:149–166.

PLUMB, O. A., G. A. SPOLEK, AND B. A. OLMSTEAD. 1985. Heat and mass transfer in wood during drying. Int. J. Heat Mass Transfer 28(9):1669–1678.

SAHA, R. S., AND R. P. TRIPATHI. 1981. Effect of temperature on the soil-water content-suction relationship. Indian Soc. Soil Sci. 29(2):143–147.

SEBASTIAN, L. P., W. A. CÔTÉ, AND C. SKAAR. 1965. Relationship of gas phase permeability to ultrastructure of white spruce wood. Forest Prod. J. 15:394–404.

SIAU, J. F. 1983. Chemical potential as a driving force for nonisothermal moisture movement in wood. A model for unsteady-state gas flow in the longitudinal direction in wood. Wood Sci. Technol. 17(2):101–105.

———. 1992. Nonisothermal diffusion model based on irreversible thermodynamics. Wood Sci. Technol. 26(5): 325–328.

———. 1995. Wood: influence of moisture on physical properties. Dept. of Wood Sci. and Forest Prod. Virginia Polytechnic Institute and State University. Blacksburg, VA. 227 pp.

SKAAR, C. 1988. Wood-water relations. Springer-Verlag, New York, NY. 283 pp.

———, AND N. KURODA. 1985. Application of irreversible thermodynamics to moisture transport phenomena in wood. Pages 152–158 *in* Proc. North American Drying Symposium. Mississipi Forest Products Utilization Laboratory.

STANISH, M. A., G. S. SCHAJER, AND F. KAYIHAN. 1986. A

mathematical model of drying for hygroscopic porous media. AICHE J. 32(8):1301–1311.

STONE, J. E., AND A. M. SCALLAN. 1967. The effect of component removal upon the porous structure of the cell wall of wood II. Swelling in water and the fiber saturation point. Tappi 50(10):496–501.

THOMAS, H. R., R. W. LEWIS, AND K. MORGAN. 1980. An application of finite element method to the drying of timber. Wood Fiber 11(4):237–243.

TREMBLAY, C., A. CLOUTIER, AND Y. FORTIN. 1996. Moisture content-water potential relationship of red pine sapwood above the fiber saturation point and the determination of the effective pore size distribution. Wood Sci. Technol. 30:361–371.

VIKTORIN, Z., AND B. ČERMÁK. 1977. Rozbor problematiky a určování chemického potenciálu vlhkostidřeva. Drevársky Výskum 22:235–259.

WHEELER, E. A. 1982. Ultrastructural characteristics of red maple (*Acer rubrum* L.) wood. Wood Fiber 14(1):43–53.

WHITAKER, S. 1977. Simultaneous heat, mass and momentum transfer in porous media: a theory of drying. Pages 119–203 *in* J. P. Hartnett and T. F. Irvine Jr., eds. Advances in heat transfer, vol. 13, Academic Press, New York, NY.